Volume 18 | Number 42 | 14 November 2016 | Pages 8127–8322

CrystEngComm

www.rsc.org/crystengcomm

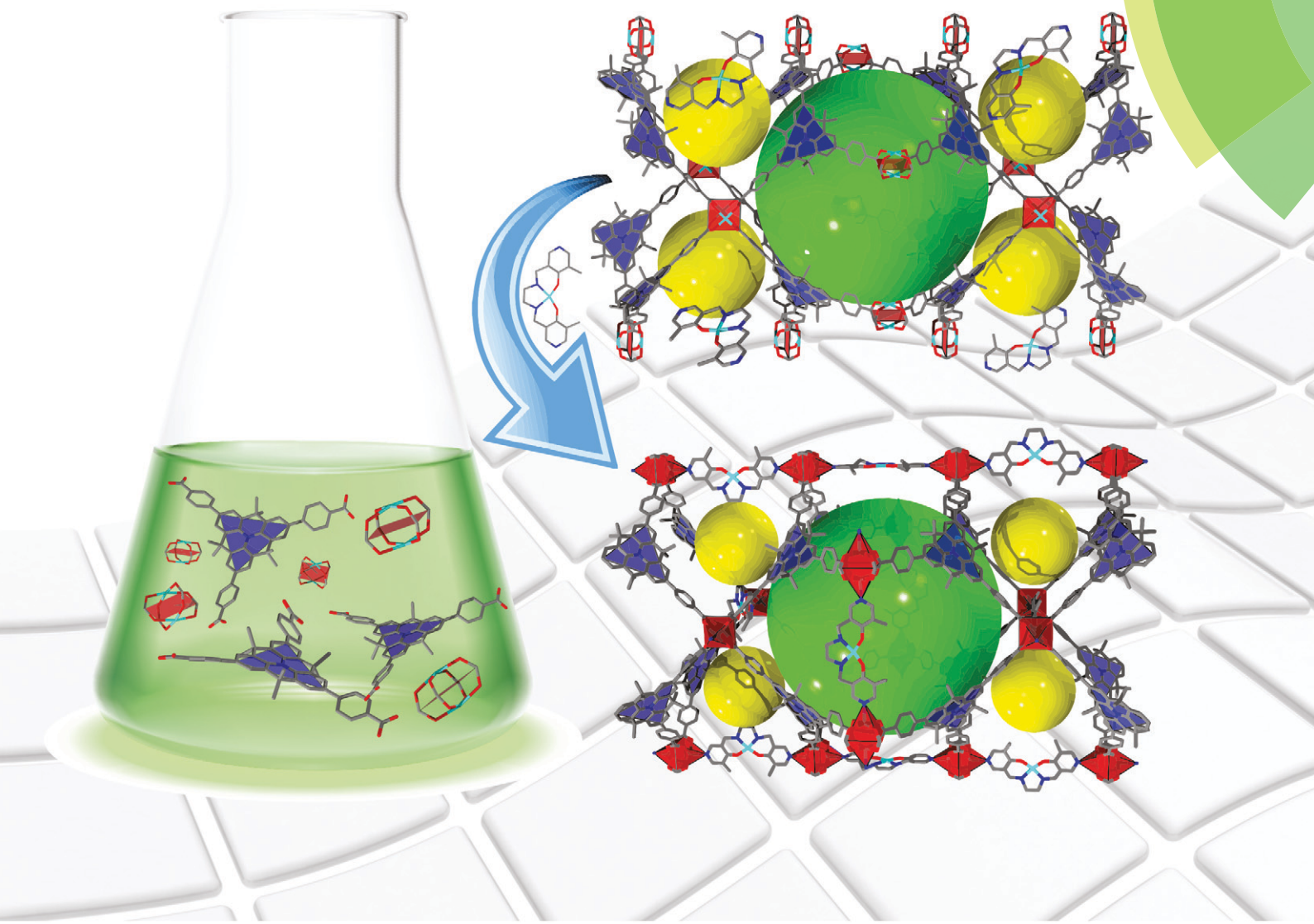

ROYAL SOCIETY OF CHEMISTRY

PAPER
Stefan Kaskel *et al.*
Topological control of 3,4-connected frameworks based on the Cu_2-paddle-wheel node: **tbo** or **pto**, and why?

175 YEARS

CrystEngComm

PAPER

View Article Online
View Journal | View Issue

Cite this: *CrystEngComm*, 2016, **18**, 8164

Topological control of 3,4-connected frameworks based on the Cu_2-paddle-wheel node: tbo or pto, and why?†‡

Philipp Müller,[a] Ronny Grünker,[ab] Volodymyr Bon,[a] Martin Pfeffermann,[d] Irena Senkovska,[a] Manfred S. Weiss,[c] Xinliang Feng[b] and Stefan Kaskel*[a]

Received 7th July 2016,
Accepted 12th August 2016

DOI: 10.1039/c6ce01513a

www.rsc.org/crystengcomm

Two trigonal tritopic ligands with different conformational degree of freedom: conformationally labile H_3tcbpa (tris((4-carboxyl)phenylduryl)amine) and conformationally obstructed H_3hmbqa (4,4′,4″-(4,4,8,8,12,12-hexamethyl-8,12-dihydro-4*H*-benzo[9,1]quino-lizino[3,4,5,6,7-defg]acridine-2,6,10-triyl)-tribenzoic acid) are assembled with square-planar paddle-wheel nodes with the aim of selective engineering of the frameworks with **tbo** and **pto** underlying net topologies. In the case of H_3tcbpa, both topological types were obtained forming non-interpenetrated MOFs namely DUT-63 (**tbo**) and DUT-64 (**pto**). Whereas synthesis of DUT-63 proceeds under typical conditions, formation of DUT-64 requires an additional topology directing reagent (topological modifier). Solvothermal treatment of the conformationally hindered H_3-hmbqa ligand with the Cu-salt results exclusively in DUT-77 material, based on the single **pto** net. The possibility to insert the salen based metallated pillar ligand into networks with **pto** topology post-synthetically results in DUT-78 and DUT-79 materials (both **ith-d**) and opens new horizons for post-synthetic insertion of catalytically active metals within the above-mentioned topological type of frameworks.

Introduction

Metal–organic frameworks (MOFs) are a class of crystalline porous solids constructed from inorganic and organic building units by modular approach[1] possessing a very bright application potential.[2,3] By combination of the topological and isoreticular synthesis approaches, an infinite number of frameworks with target structure and properties could be theoretically predicted.[4,5] However, an unambiguous prediction is not always possible, due to the plurality of factors influencing the MOF formation, namely framework interpenetration, secondary building unit (SBU) assembly formed under defined synthetic conditions, solvent or ligand degradation processes, preferred ligand conformation in solution *etc.*

Nevertheless, crystal engineering plays a key role in the synthesis of novel MOF materials for desired applications. Nowadays, the reticular chemistry offers several approaches for the synthesis of MOF materials with specific textural properties that are based on the control of the underlying topology of the framework.[6,7] In this regards, tritopic ligands are very attractive systems due to the restricted topological diversity of resulting structures, especially if the latter is combined with a square-planar 4-connected inorganic nodes.[8–10]

Thus, application the isoreticular approach to the HKUST-1 (ref. 11) structure (**tbo** topology) by expanding the btc^{3-} (1,3,5-benzenetricarboxylate) ligand to btb^{3-} (btb – 1,3,5-benzenetribenzoate) has first led to the interpenetrated structure of MOF-14 (ref. 12) with two interwoven **pto** type frameworks in the structure. Just a slight modification of the synthesis conditions by adding small amounts of pyridine leads to the formation of DUT-33 and DUT-34 materials (DUT – Dresden University of Technology) consisting of doubly interpenetrated **tbo** and single **pto** frameworks, respectively.[8,13] The non-interpenetrated **tbo** net could be achieved only by using the H_3btb ligand with bulky substituents at peripheral phenyl ring[14] or triazine based H_3tatb (H_3tatb – 4,4′,4″-*s*-triazine-2,4,6-triyltribenzoate).[15,16] In both cases the peripheral phenyl rings are nearly coplanar with the central one. Further isoreticular expansion of the H_3btb to the H_3bbc (H_3bbc – 4,4′,4″-(benzene-1,3,5-triyl-tris(benzene-4,1-diyl))-tribenzoic acid) results in the MOF-399 structure with **tbo**

[a] *Department of Inorganic Chemistry, Technische Universität Dresden, Bergstrasse 66, D-01062 Dresden, Germany. E-mail: Stefan.Kaskel@tu-dresden.de*
[b] *Center for Advancing Electronics Dresden, Technische Universität Dresden, Bergstrasse 66, D-01062 Dresden, Germany*
[c] *MX Group, Institute for Soft Matter and Functional Materials, Helmholtz-Zentrum Berlin für Materialien und Energie, Albert-Einstein-Str. 15, 12489 Berlin, Germany*
[d] *Max Planck Institute for Polymer Research, Ackermannweg 10, 55128 Mainz, Germany*

† Dedicated to Professor Klaus K. Unger on the occasion of his 80th birthday.

‡ Electronic supplementary information (ESI) available: PXRD patterns, ^{1}H-NMR-spectra, nitrogen physisorption isotherms. CCDC 1480874–1480878. For ESI and crystallographic data in CIF or other electronic format see DOI: 10.1039/c6ce01513a

underlying topology.[17] Very recently, using even longer bteb^{3-} (H_3bteb – 1,3,5-benzene-trisethynylbenzoic acid) as a ligand and slightly different synthetic conditions, Schmitt and co-workers succeed in the synthesis of two MOFs isoreticular to MOF-399, namely TCM-4 and TCM-8 containing interpenetrated **tbo** and **pto** frameworks, respectively.[18] Obviously, an alkyne functional group, introduced between the central and peripheral phenyl ring, leads to the minimization of the energy difference between two ligand conformations, favouring the particular topology. Calculations demonstrated that the potential pore volume, surface area and N_2 uptake capacity of the **tbo** structure, TCM-8, are substantially higher than those of the **pto** counterpart.

Schmid and co-workers have theoretically screened possible network topologies of copper paddle-wheel based systems with the tritopic linkers btc^{3-} and btb^{3-} with respect to their relative stability.[19] Their results demonstrate, that the intrinsic conformational preferences of the building blocks often dictate the network topology formed.

In order to support this thesis experimentally, ligands with a fixed conformation would be ideal model systems to provide some evidence. Having this in mind, we have conceptually developed and synthesized two trigonal ligands: H_3-tcbpa (H_3tcbpa – tris((4-carboxyl)phenylduryl)amine) and H_3-hmbqa (H_3hmbqa – 4,4′,4″-(4,4,8,8,12,12-hexamethyl-8,12-dihydro-4*H*-benzo[9,1]quino-lizino[3,4,5,6,7-defg]acridine-2,6,10-triyl)tribenzoic acid) (Fig. 1) and combined them with Cu_2-paddle-wheels, using an appropriate copper source in the synthesis.

The H_3tcbpa ligand has been already widely used for the design and synthesis of various MOFs,[20–28] including those based on the paddle-wheel SBU,[23,29] however neither **tbo** nor **pto** type structures are reported up to now. The H_3hmbqa ligand could be viewed as a chemically fixed conformation of the first one, since their internal phenyl rings are connected to the quasi-planar core by three methylene bridges. By variation of the synthesis conditions, both **tbo** (DUT-63) and **pto** (DUT-64) structures could be obtained with H_3tcbpa, which confirms the conformational lability of the latter. In contrast, the rigid core of the H_3hmbqa ligand forces the formation of the **pto** structure (DUT-77) exclusively. Moreover, using nitrogen functionalized metal–salen-complex, (further named as Cu(salen), Fig. 1, formed by reaction of 5-methyl-4-oxo-1,4-dihydropyridine-3-carbaldehyde with ethylenediamine and copper nitrate) as a crosslinking ligand, the frameworks of **pto** topology could be post-synthetically transformed into framework with **ith-d** underlying topology.

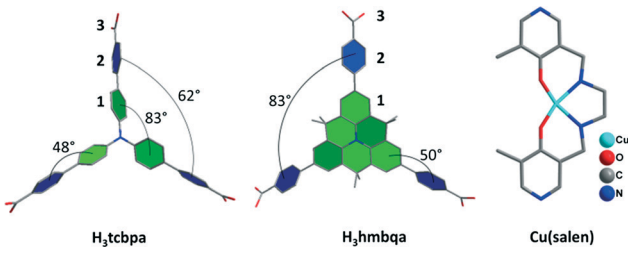

Fig. 1 Geometrically optimized models of H_3tcbpa (left) and H_3hmbqa (middle). Cu(salen) complex used as cross-linker (right).

Experimental part

All commercially available chemicals and solvents were used as purchased without further purification. Silica gel for column chromatography with particle sizes of 0.063–0.200 mm and SIL G/UV254 ALUGRAM® aluminium sheets for thin layer chromatography were purchased from Macherey-Nagel. Reactions under inert gas (Argon 4.6, Linde AG) were done with standard Schlenk techniques.

Synthesis of H_3tcbpa

H_3tcbpa ligand was synthesized using slightly modified procedure described in ref. 20. Bromine (7.51 mL, 147 mmol, 3 eq.) dissolved in chloroform (20 mL) was injected to a solution of triphenylamine (12.00 g, 0.049 mol) in chloroform (75 mL) over a time period of 30 min at 0 °C. After stirring the solution at room temperature for additional 30 min the solvent was evaporated. The resulting solid was dissolved in a small amount of chloroform and 200 mL of hot ethanol was added. After the solution is cooled in an ice bath, tris(4-bromophenyl)amine crystallizes as colourless needles. (Yield: 22.94 g, 476 mmol, 97%). ^{1}H-NMR (*CDCl*$_3$, 500 MHz): δ (in ppm): 6.91 (d, 6H), 7.34 (d, 6H). ^{13}C-NMR (*CDCl*$_3$, 125 MHz): δ (in ppm): 116.04 (C_q), 125.60 (CH), 132.50 (CH), 146.03 (C_q).

Tris(4-bromophenyl)amine (5.00 g, 10.37 mmol), 4-methoxycarbonylphenylboronic acid (11.20 g, 62.24 mmol, 6 eq.), palladium(II) acetate (0.140 g, 0.62 mmol, 6 mol%), triphenylphosphine (0.544 g, 2.08 mmol, 20 mol%) and Cs_2CO_3 (20.28 g, 62.24 mmol, 6 eq.) were stirred at reflux in dry tetrahydrofuran for 72 h under argon atmosphere. The yellow suspension was cooled down to room temperature and the inorganic salts were removed by filtration through a pad of Celite®. After removal of the solvent in vacuum, the resulting yellow-brown solid was dissolved in DCM and washed with water. After drying of the organic phase the solvent was removed by evaporation. The resulting yellow needles were filtered and dried under vacuum. (Yield: 6.573 g, 10.15 mmol, 98%). ^{1}H-NMR (*CDCl*$_3$, 500 MHz): δ (in ppm): 3.94 (s, 9H), 7.26 (d, 6H), 7.58 (d, 6H), 7.66 (d, 6H), 8.10 (d, 6H). ^{13}C-NMR (*CDCl*$_3$, 125 MHz): δ (in ppm): 52.13 (CH_3), 124.53 (CH), 126.47 (CH), 128.20 (CH), 128.52 (C_q), 130.16 (CH), 134.59 (C_q), 144.79 (C_q), 147.26 (C_q), 167.00 (C_q).

In a round bottom flask tris(4′-methoxycarbonylbiphenyl)-amine (6.10 g, 9.41 mmol) was dissolved in 200 mL tetrahydrofuran and a solution of KOH (10.56 g, 188 mmol, 20 eq.) in 50 mL H_2O was added. This mixture was refluxed for 18 h. After cooling down to room temperature, THF was evaporated and 300 mL H_2O was added to dissolve all obtained solid. The water phase was acidified with conc. HCl until no further precipitate was detected. The yellow solid was collected by filtration, washed with water, small amounts of tetrahydrofuran

and diethyl ether and dried under vacuum. (Yield: 5.09 g, 8.40 mmol, 89%). ^{1}H-NMR (*DMSO-d*$_6$, 500 MHz): δ (in ppm): 7.21 (d, 6H), 7.75 (d, 6H), 7.80 (d, 6H), 8.00 (d, 6H), 12.97 (br, 3H). ^{13}C-NMR (*DMSO-d*$_6$, 125 MHz): δ (in ppm): 124.34 (CH), 126.27 (C_q), 128.23 (CH), 129.17 (C_q), 130.00 (CH), 133.66 (C_q), 143.56 (C_q), 146.80 (C_q), 167.14 (C_q).

Synthesis of bpta (bpta – 3,6-dibi(pyridin-4-yl)-1,2,4,5-tetrazine) (bpta)

4-Cyanopyridine (20.80 g, 200 mmol) was refluxed for 5 h in hydrazine monohydrate (39 mL, 40.06 g, 800 mmol, 4 eq.). After cooling the solution to 0 °C the orange 1,4-dihydro-1,2,4,5-tetrazine intermediate precipitated. After filtration and washing of the solid with diethyl ether, it was dissolved in 210 mL glacial acetic acid/H_2O mixture (4 : 3) and sodium nitrite solution (15.20 g, 220 mmol, 1.1 eq. in 25 mL H_2O) was added dropwise at 0 °C. After 1 h at 0 °C the solution was neutralized with ice-cooled conc. ammonia and the resulting solid was filtered and recrystallized from ethanol to get the desired product as violet crystals. (Yield: 4.85 g, 31.46 mmol, 21%). ^{1}H-NMR (*CDCl*$_3$, 500 MHz): δ (in ppm): 8.52 (d, 4H), 8.97 (d, 4H). ^{13}C-NMR (*CDCl*$_3$, 125 MHz): δ (in ppm): 121.41 (CH), 138.63 (C_q), 151.31 (CH), 163.76 (C_q).

Synthesis of Cu(salen)$(NO_3)_2$

Cu(salen)$(NO_3)_2$ was synthesized using slightly modified procedure described before.[30] Diethyl-2-(ethoxymethylen)-malonate (62.20 g, 287 mmol, 42.5 mL) was dissolved in 115 mL methanol and *n*-propylamine (23.77 g, 403 mmol, 33 mL, 1.4 eq.) dissolved in 30 mL methanol was added dropwise under stirring. The solution was stirred for additional 30 min, afterwards methanol was evaporated under reduced pressure and the obtained diethyl-2-((propylamino)methylene)malonate was dried under vacuum overnight (yield: 65.8 g, 287 mmol, 100%). ^{1}H-NMR (*CDCl*$_3$, 500 MHz): δ (in ppm): 0.95 (t, 3H), 1.27 (t, 3H), 1.32 (t, 3H), 1.62 (sx, 2H), 4.16 (q, 2H), 4.21 (q, 2H), 7.98 (d, 1H), 9.21 (br, 1H, NH). ^{13}C-NMR (*CDCl*$_3$, 125 MHz): δ (in ppm): 10.94 (CH_3), 14.33 (CH_3), 14.43 (CH_3), 23.94 (CH_2), 51.45 (CH_2), 59.53 (CH_2), 89.17 (C_q), 160.07 (C_q), 166.19, 169.46 (C_q).

Diethyl-2-((propylamino)methylene)malonate (10.00 g, 43.60 mmol) was dissolved in 100 mL THF. The solution was introduced in small portions (4 mL each) into a vertical heated reaction column (420 °C) under vacuum. The column was filled with glass spheres, glass wool, and sand (Fig. S15‡). The crude product was collected together with THF in a cooling trap. After termination of the reaction, the solid 5-methyl-4-oxo-1,4-dihydropyridine-3-carbaldehyde was collected by flushing the vessel with ethanol. Afterwards ethanol was evaporated and the product was washed with diethyl ether and dried under vacuum (yield: 3.38 g, 24.85 mmol, 57%). ^{1}H-NMR (*DMSO-d*$_6$, 500 MHz): δ (in ppm): 1.87 (s, 3H), 7.64 (s, 1H), 8.09 (s, 1H), 10.10 (s, 1H), 11.88 (br, 1H, NH). ^{13}C-NMR (*DMSO-d*$_6$, 125 MHz): δ (in ppm): 13.11 (CH_3), 120.87 (C_q), 130.55 (C_q), 135.27 (CH), 140.17 (CH), 177.44 (C_q), 190.30 (CH).

5-Methyl-4-oxo-1,4-dihydropyridine-3-carbaldehyde (1.50 g, 11.00 mmol) was dissolved in 37 mL ethanol and ethylenediamine (0.330 g, 5.5 mmol, 0.5 eq.) dissolved in 15 mL ethanol was added dropwise. The solution was refluxed for 2 h. After cooling down to room temperature, $Cu(NO_3)_2{\cdot}3H_2O$ (1.32 g, 5.50 mmol, 0.5 eq.) dissolved in 20 mL ethanol was added dropwise. The resulted solid was filtered, washed with ethanol and dried under vacuum (yield: 2.44 g, 4.92 mmol, 89%). Elemental analysis: $(CuC_{16}O_2N_4H_{16})(NO_3)_2{\cdot}0.65H_2O$ (495.58 g mol^{-1}): calcd.: C, 38.7; H, 3.5; N, 16.9. Found: C, 38.9; H, 3.7; N 17.0.

Synthesis of H_3hmbqa

2,6,10-Tribromo-4,4,8,8,12,12-hexamethyl-8,12-dihydro-4*H*-benzo-[9,1]quinolizino[3,4,5,6,7-defg]acridine[31] (1.00 g, 1.66 mmol, 1 eq.) was added to 4-(methoxycarbonyl)phenylboronic acid (3.59 g, 19.93 mmol, 12 eq.), 20.0 mL 2 M aqueous potassium carbonate solution and 75 mL THF under argon atmosphere at room temperature. Tetrakis(triphenylphosphine)-palladium(0) (0.288 g, 0.249 mmol, 0.15 eq.) was added slowly under stirring and the reaction mixture was heated subsequently to 65 °C for 2 d. After cooling to room temperature, water was added to quench the reaction. The mixture was extracted with DCM and the organic phase was separated. After removing the solvent, the solid was subjected to column chromatography (flash gel, eluent: DCM/MeOH/Et_3N = 1000/10/7). The resulting yellow powder was added to 12 mL of a 2 M KOH solution in ethanol. The reaction mixture was heated to 40 °C for 16 h. A pH value of 6 was adjusted with concentrated HCl. The precipitate was filtered and the filtrate was extracted with ethyl acetate. The organic phase was removed and combined with the precipitate. After the solvent was removed, the solid was washed with water and hexane to yield 0.267 g (0.368 mmol, 22%) of H_3hmbqa as a yellow powder. Melting point: 378 °C (decomposition); ^{1}H-NMR (700 MHz, *DMSO-d*$_6$): δ = 12.93 (bs, 3H), 8.04 (d, 6H), 7.96 (d, 6H), 7.85 (s, 6H), 1.77 (s, 18H); ^{13}C-NMR (176.0 MHz, *DMSO-d*$_6$): δ (in ppm): 33.39 (CH_3), 35.59 (C_q), 122.67 (CH), 126.32 (CH), 129.01 (C_q), 130.42 (C_q), 130.62 (C_q), 133.70 (C_q), 143.89 (C_q), 167.24 (C_q); MS (HR ESI-TOF, positive): *m*/*z* 725.2761 $[M]^+$ (calc. for $C_{48}H_{39}NO_6$ 725.2777).

Synthesis of $Cu_3(tcbpa)_2(H_2O)_3$ (DUT-63)

$Cu(NO_3)_2{\cdot}3H_2O$ (30 mg, 0.124 mmol), H_3tcbpa (10.4 mg, 0.017 mmol) and a drop of glacial acetic acid (*ca.* 4.3 μL) were dissolved in 2 mL DMF by sonication. The mixture was heated to 80 °C in a Pyrex tube. After 24 h the hot mother liquor was taken off by syringe and the octahedral crystals were washed with fresh DMF (8 mL) (yield: 6 mg, 0.004 mmol, 50%). $Cu_3(tcbpa)_2(H_2O)_3(DMF)_{45}(H_2O)_{12}$ ($C_{213}H_{393}O_{72}N_{47}Cu_3$) (4955.31 g mol^{-1}), confirmed by ^{1}H-NMR.

Synthesis of $Cu_2(tcbpa)_{4/3}$ (DUT-64)

$Cu(NO_3)_2{\cdot}3H_2O$ (30 mg, 0.124 mmol, 7.3 eq.), H_3tcbpa (10.4 mg, 0.017 mmol) were dissolved in 2 mL DMF by

sonification. Eight drops of glacial acid (*ca.* 35 μL) were added. Separately dissolved bpta (4 mg, 0.017 mmol, 1 eq.) in 2 mL DMF was added. The mixture was heated to 80 °C in a Pyrex tube for 24 h. After cooling to room temperature, the solvent was replaced by fresh DMF and exchanged to acetone over three days (three times per day). Finally the crystals of DUT-64 were dried with supercritical carbon dioxide (yield: 7.12 mg, 0.007 mmol, 57%). $Cu_2(tcbpa)_{4/3}(EtOH)_{0.17}$ ($C_{52.34}H_{32.85}O_{8.17}N_{1.33}Cu_2$) (938.13 g mol^{-1}), confirmed by ^{1}H-NMR (Fig. S7, ESI‡).

Synthesis of $Cu_2(hmbqa)_{4/3}$ (DUT-77)

$Cu(NO_3)_2{\cdot}3H_2O$ (30 mg, 0.124 mmol, 7.3 eq.), H_3hmbpa (12.5 mg, 0.017 mmol) were dissolved in 2 mL DMF by signification. The mixture was heated to 80 °C in a Pyrex tube for 24 h. After cooling to room temperature, the solvent was replaced by fresh DMF and exchanged to acetone over three days (three times per day). Finally the crystals of DUT-77 were dried with supercritical carbon dioxide (yield: 7.33 mg, 0.0065 mmol, 51%). $Cu_2(hmbqa)_{4/3}$ ($C_{64}H_{48}O_8N_{1.33}Cu_2$) (1090.72 g mol^{-1}), confirmed by ^{1}H-NMR (Fig. S8, ESI‡).

Synthesis of $Cu_2(tcbpa)_{4/3}(Cu(salen))$ (DUT-78)

To the washed crystals of DUT-64, $Cu(salen)(NO_3)_2$ solution (15 mg, 0.04 mmol dissolved in 12 mL DMF) was added and the mixture was heated to 80 °C for 5 days. After cooling to room temperature, the solvent was replaced by fresh DMF and exchanged to acetone over three days (three times per day). Finally the crystals of DUT-78 were dried with supercritical carbon dioxide (yield: 6.84 mg, 0.0055 mmol, 43%). $Cu_2(tcbpa)_{4/3}(Cu(salen))_{0.87}(EtOH)_{0.11}$ ($C_{66.14}H_{46.47}O_{9.85}N_{4.88}Cu_{2.87}$) (1249.48 g mol^{-1}), confirmed by ^{1}H-NMR (Fig. S9, ESI‡).

Synthesis of $Cu_2(hmbqa)_{4/3}(Cu(salen))$ (DUT-79)

To the washed crystals of DUT-77, $Cu(salen)(NO_3)_2$ solution (15 mg, 0.04 mmol dissolved in 12 mL DMF) was added and the mixture was heated to 80 °C for 5 days. After cooling to room temperature, the solvent was replaced by fresh DMF and exchanged to acetone over three days (three times per day). Finally the crystals of DUT-79 were dried with supercritical carbon dioxide (yield: 8.07 mg, 0.0053 mmol, 42%). $Cu_2(hmbqa)_{4/3}(Cu(salen))_{1.25}(EtOH)_{0.01}$ ($C_{84.02}H_{68.06}O_{10.51}N_{6.33}Cu_{3.25}$) (1540.95 g mol^{-1}), confirmed by ^{1}H-NMR (Fig. S10, ESI‡).

Physical measurements

The elemental analyses for C, H, N were performed with CHNS 932 analyzer (LECO) or EA 3000 Euro Vector (HEKAtech). Theoretical calculations of surface area, pore volume and pore limiting diameter were performed using Zeo++ software.[32]

Single crystal X-ray diffraction

All datasets were collected at Helmholtz-Zentrum Berlin für Materialien und Energie on BL-14.2 or BL-14.3 beamlines at BESSY-MX, equipped with a Mar MX-225 CCD detector (Rayonics, Illinois).[33] Images were recorded at room temperature using φ-scan technique with a scan width of 1° and an exposure time of 1.2 s per frame. Datasets were integrated and scaled with CCP4i software package.[34] Structures were solved by direct methods and refined in anisotropic approximation for all non-hydrogen atoms by full-matrix least squares on F^2 using SHELXTL program package.[35] The hydrogen atoms were placed in geometrically calculated positions and refined using a "riding" model. Cu(salen) ligand in the crystal structure of DUT-78 is disordered over two positions with occupancies 0.64 and 0.36, correspondingly. In the part with lower occupancy, only Cu atom could be localized from the difference Fourier map, whereas nitrogen and carbon atoms could not be localized unambiguously. The lattice solvent molecules as well as terminal ligands could not be located from difference Fourier map due to disorder in the highly symmetric space group. The influence of disordered solvent molecules on the reliability factors was eliminated by applying the SQUEEZE procedure, implemented in PLATON program.[36] Detailed experimental data for the single crystal X-ray diffraction experiments are given in Table S1.‡ CCDC-1480874–1480878 contains the supplementary crystallographic data for DUT-63, DUT-64, DUT-77, DUT-78 and DUT-79.

Crystal data for DUT-63: $C_{78}H_{48}Cu_3N_2O_{15}$, M_r = 1443.80, cubic $F432$, a = 60.910(7) Å, V = 225 978(45) Å^3, Z = 16, D_c = 0.170 g cm^{-3}, 8549 independent reflections observed, R^1 = 0.0540 ($I > 2\sigma(I)$), wR^2 = 0.1324 (all data), GOF = 0.658.

Crystal data for DUT-64: $C_{52}H_{32}Cu_2N_{1.33}O_{10}$, M_r = 962.53, cubic $Pm\bar{3}n$, a = 35.490(4) Å, V = 44 701(15) Å^3, Z = 6, D_c = 0.215 g cm^{-3}, 3055 independent reflections observed, R^1 = 0.0771 ($I > 2\sigma(I)$), wR^2 = 0.2861 (all data), GOF = 0.843.

Crystal data for DUT-77: $C_{64}H_{48}Cu_2N_{1.33}O_{10}$, M_r = 1122.78, cubic $Pm\bar{3}n$, a = 35.400(4) Å, V = 44 362(15) Å^3, Z = 6, D_c = 0.252 g cm^{-3}, 2666 independent reflections observed, R^1 = 0.1101 ($I > 2\sigma(I)$), wR^2 = 0.3458 (all data) GOF = 1.217.

Crystal data for DUT-78: $C_{68}H_{48}Cu_3N_{5.33}O_{10}$, M_r = 1290.40, cubic $Pm\bar{3}n$, a = 35.510(4) Å, V = 44 777(16) Å^3, Z = 6, D_c = 0.287 g cm^{-3}, 4827 independent reflections observed, R^1 = 0.0673 ($I > 2\sigma(I)$), wR^2 = 0.2455 (all data), GOF = 1.140.

Crystal data for DUT-79: $C_{82}H_{64}Cu_3N_{7.33}O_{10}$, M_r = 1502.69, cubic $Pm\bar{3}n$, a = 35.490(4) Å, V = 44 701(15) Å^3, Z = 6, D_c = 0.335 g cm^{-3}, 2632 independent reflections observed, R^1 = 0.0998 ($I > 2\sigma(I)$), wR^2 = 0.3243 (all data), GOF = 1.205.

Results and discussion

MOFs containing tcbpa ligand

The solvothermal reaction of $Cu(NO_3)_2$ and H_3tcbpa in DMF leads to the formation of green octahedral crystals with the composition $Cu_3(tcbpa)_2(L)_3$ (L – solvent) further named as DUT-63. Single crystal X-ray diffraction analysis reveals a

cubic F-centered lattice. The crystal structure of the framework is constructed from Cu paddle-wheels, interconnected by trigonal tcbpa^{3-} linkers forming 3D framework with **tbo** underlying topology. Thus, DUT-63 is isoreticular to HKUST-1. The phase purity of DUT-63 "as made" phase was confirmed by X-ray powder diffraction (Fig. S1, ESI‡). Similar to HKUST-1, DUT-63 has 3 types of pores with 15.5, 28.0 and 32.2 Å in diameter (Fig. 2f). According to Zeo++ program,[32] the molecules with maximal diameter of 18.9 Å could penetrate into the pores (Table 1). The geometric surface area and pore volume are 4768 m^2 g^{-1} and 4.83 cm^3 g^{-1}, respectively. Thus, the material has crystallographic porosity ranking among the most porous MOFs. Unfortunately, all attempts to remove the solvent from the pores without framework collapse failed. The reason might be in the ultra-low density of 0.17 g cm^{-3}, resulting in a high fragility of the desolvated framework. This is corroborated by a high value of solvent accessible void of 91.4% calculated from the crystal structure.

Inspired by our previous work,[37] and in order to force the formation of **ith-d** framework, a neutral linear diamine linker, namely 3,6-di(pyridin-4-yl)-1,2,4,5-tetrazine (bpta),

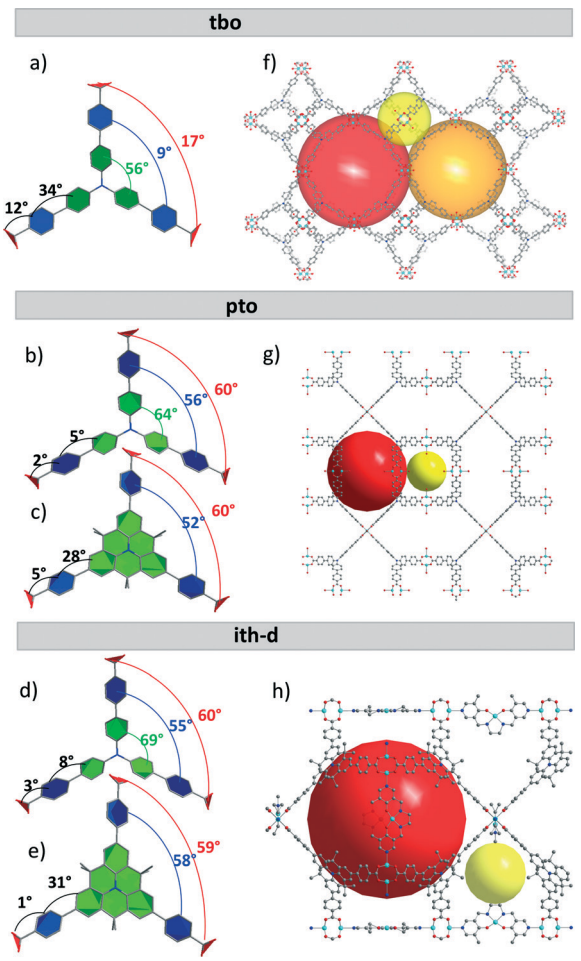

Fig. 2 Ligand conformations with dihedral angles for: a) DUT-63; b) DUT-64; c) DUT-77; d) DUT-78; e) DUT-79. Crystal structure of: f) DUT-63; g) DUT-64; h) DUT-79.

Table 1 Calculated textural properties for DUT-63, DUT-64, DUT-77, DUT-78 and DUT-79 materials

MOF	DUT-63	DUT-64	DUT-77	DUT-78	DUT-79
Topology	**tbo**	**pto**	**pto**	**ith-d**	**ith-d**
ρ_{cryst}, cm^3 g^{-1}	0.17	0.26	0.25	0.29	0.34
SAV, %	91.4	89.5	87.2	85.6	82.5
SSA, m^2 g^{-1}	4768	5817	5556	4495	4059
V_p, cm^3 g^{-1}	4.83	3.62	2.90	2.55	1.69
d_{max}, Å	32.8	26.3	25.1	24.9	25.3
d_{limit}, Å	18.9	11.9	11.7	11.8	7.9

ρ_{cryst} – crystallographic density, SAV – solvent accessible void, SSA – specific surface area, V_p – pore volume, d_{max} – maximum pore diameter, d_{limit} – limiting pore diameter.

potentially suitable for interconnection of the paddle-wheels,[38–40] was added during the synthesis. This resulted in the formation of cuboctahedral green crystals, crystallizing in the *Pm*$\bar{3}$*n* space group, according to the single crystal X-ray diffraction analysis. The crystal structure of this novel material (DUT-64) adopts a single 3,4-binodal framework with **pto** topology (Fig. 2g). Interestingly, the bpta ligand was not found neither during the structure solution from the X-ray data, nor during the ^{1}H-NMR analysis after digestion of DUT-64 (Fig. S7, ESI‡). It seems, bpta serves in this case only as a topological modifier for the structure formation, but does not integrate into the structure. Similar observations were made by Schmitt and co-workers during the synthesis of TCM-4.[18] In this case, 4,4-bipyridine serves as topology directing agent to enable the formation of the **pto** net.

The pore system of DUT-64 involves two types of pores (Fig. 2g). The large mesopore with 26.3 Å in diameter is built from twelve paddle-wheel units, arranged icosahedral and interconnected by eight tcbpa^{3-} linkers. The mesopores are connected by twelve micropores with five pentagonal pore windows each. The micropores with diameter of 16.5 Å are formed by four SBUs and four tcbpa^{3-} linkers. The solvent accessible volume, calculated using PLATON is lower, than that of DUT-63 and amounts to 89.5%. Despite of lower pore volume, DUT-64 exhibits a higher geometrical surface area of 5817 m^2 g^{-1} (Table 1). Due to the topological reasons, the pore limiting diameter for the DUT-64 structure amounts to 11.9 Å and therefore is significantly lower in comparison to DUT-63.

As the bpta molecule seems to be too long for paddle-wheel crosslinking (N···N distance 11.1 Å), a shorter neutral diamine ligand (Cu(salen), N···N distance 10.82 Å,[30] Fig. 1) was used for post-synthetic incorporation into the DUT-64 yielding a MOF with **ith-d** topology (DUT-78). The crystallinity and phase purity of as synthesised sample was proved by PXRD (Fig. S4, ESI‡). The successful incorporation of Cu(salen) was proven by ^{1}H NMR in solution after dissolving the MOF (Fig. S9, ESI‡). To confirm the coordination mode of the Cu(salen), the single crystal of DUT-78 was subjected to the single crystal X-ray diffraction at synchrotron. Refinement of the structure shows the incorporation of the

Cu(salen) ligand unambiguously. The interconnection of paddle-wheels in the crystal structure caused only minimal changes in the conformation of the $tcbpa^{3-}$ linker (Fig. 2b and d, Table 2). It has also nearly no influence on the pore accessibility. Thus, the theoretical pore size distribution, shows nearly no influence of the cross-linking on the size of the large pore. The small pore size ranged from 8.8 (in DUT-79) to 16.5 Å (in DUT-64) depending on the linkers (Fig. S6, ESI‡). The only parameters that are slightly decreased due to the functionalization are geometrical surface area and pore volume (Table 1).

Unfortunately all attempts to preserve the framework integrity during the removing of the solvent molecules failed (Fig. S13, ESI‡). Presumably, the weak spot in this structure is a central nitrogen atom that could distort from sp^2 planar configuration under the harsh conditions that lead to the structural collapse. In prospective, functionalization of the MOF by neutral metallo-ligand is advantageous for catalysis, since not only Cu, but also other catalytically active metals such as Ni, Pd, Pt *etc.* can be introduced into this highly accessible porous system.

Conformational considerations

The geometry of both ligands was analysed using models, obtained by geometrical optimization of the H_3tcbpa and H_3hmbqa molecules by Forcite tools (UFF force field), implemented in Materials Studio 5.0 software.[41] Since dihedral angles between the outer phenyl rings in the trigonal ligand are mostly responsible for the formation of the framework with **tbo** or **pto** underlying topology,[17] we analysed these angles in the optimized linker models (Fig. 1) in comparison to those found in the DUT-63 and DUT-64 (Fig. 2, Table 2). Thus, the dihedral angle between the outer and inner phenyl rings in H_3tcbpa is equal to the interplanar angle between the outer rings and core plane in H_3hmbqa. Similarly, the interplanar angle between the inner rings in H_3tcbpa is identical to the interplanar angle between the outer rings in H_3hmbqa. At the same time, the H_3tcbpa has one additional degree of rotation and therefore a larger potential for topological diversity in combination with paddle-wheel units.

According to Furukawa *et al.* the formation of **tbo** net is possible if all three carboxylates in the linker do not show significant twist angles between them.[17] The detailed analysis of the geometry in the coordinated tcbpa linker shows that the dihedral angle between carboxylates in DUT-63 (**tbo**) is only 17° that completely match with the previous statement. The dihedral angle between two peripheral phenyl rings 1 and 2 is 34° (Fig. 2a, Table 2). The ring 2 and carboxylate group are nearly coplanar, with dihedral angle of 12° between them. It should be mentioned that some attempts to combine the copper paddle-wheels with $tcbpa^{3-}$ were reported by Shi *et al.*[23] however resulting in a 2D catenated structure.

The detailed analysis of the linker conformation in DUT-64 shows a notable difference in comparison with the latter in DUT-63 structure. Thus, the peripheral phenyl rings 1 and 2 as well as phenyl ring 2 and carboxylate group are nearly co-planar with dihedral angles of 5° and 2°, correspondingly (Table 2, Fig. 2b). Consequently, the dihedral angle between the carboxylates in the ligand is defined mostly by the angle between phenyl rings 1 and 1′, which is critical for the formation of the certain framework topology. As a result, the dihedral angle between carboxylates of 60° leads to the formation of the **pto** net (Table 2, Fig. 2b).

Thus, due to the conformational flexibility of the H_3tcbpa ligand, the assembly with the Cu_2 paddle-wheels leads to the formation of either **tbo** or **pto** nets (DUT-63 and DUT-64, respectively), depending on the synthesis conditions.

Topological control

For a better control of the topology by linker conformation, a novel tritopic ligand namely H_3hmbqa with similar distance between carboxylates but a quasi-planar inner core and restricted conformational flexibility in comparison with H_3tcbpa ligand was synthesized. In many cases, the **pto** topology is more beneficial in comparison to **tbo**, because of the possibility to crosslink the paddle-wheel with additional neutral ligand to achieve **ith-d** topology (as shown for DUT-64/DUT-78). Such crosslinking opens the possibility to stabilize the framework (as in the case of DUT-23 and DUT-34),[8] as well as to incorporate additional functionalities into the open porous framework, such as catalytic centers, chirality (DUT-24),[8] semiconductivity, or luminescence.[8,37,42]

The solvothermal treatment of the H_3hmbqa with $Cu(NO_3)_2$ in DMF (independently of the presence or absence of bpta as topological modulator) leds to the formation of the green cuboctahedral crystals of DUT-77. Single crystal X-ray diffraction analysis confirms the expected structure, isoreticular to DUT-64 with similar unit cell parameters and the **pto** underlying topology. The phase purity of the bulk sample was confirmed by PXRD measurements (Fig. S3, ESI‡). The digestion ^{1}H NMR shows the presence of the H_3hmbqa ligand exclusively (Fig. S8, ESI‡). The detailed analysis of the

Table 2 Dihedral angles between the phenyl rings and carboxylates for ligand models and crystal structures

	H_3hmbqa	H_3tcbpa	DUT-63 (**tbo**)	DUT-64 (**pto**)	DUT-77 (**pto**)	DUT-78 (**ith-d**)	DUT-79 (**ith-d**)
1–1′	—	83	56	64	—	69	
1–2	50	48	34	5	28	8	31
2–2′	83	62	9	56	52	55	58
2–3	0	0	12	2	5	3	1
3–3′	83	62	17	60	60	60	59

ligand conformation shows a dihedral angle between the carboxylic groups of 60°, which is close to that in DUT-64. This angle is of paramount importance for the formation of the **pto** net. The planarity of the inner core forces the outer phenyl ring to twist on 28°.

The similarity in size and geometry of the ligand, combined with the same topology of the framework, results in very similar textural properties of DUT-77 and DUT-64 structures calculated from the crystal structural data. However, because of the bulky and rigid core of the $hmbqa^{3-}$ linker in DUT-77, all parameters involving solvent accessible void, theoretical surface area, total pore volume and pore dimensions have slightly lower values.

An approach analogous to that applied to DUT-64 was used for post-synthetic cross-linking of the paddle-wheels by Cu(salen) complex in DUT-77. The resulting material, DUT-79, with **ith-d** topology shows nearly no conformational changes in $hmbqa^{3-}$ linker in comparison to the parent DUT-77 (Table 2, Fig. 2c and e). The incorporation of the ligand was proven by single crystal X-ray diffraction analysis (Table S1‡) and ^1H NMR techniques (Fig. S10, ESI‡).

Nitrogen adsorption experiments

To study the gas accessible porosity of the investigated frameworks, all samples were desolvated using supercritical CO_2 drying. Unfortunately it was not possible to preserve framework integrity completely during the solvent removal. According to the XRD analysis, all compounds are amorphous after activation (Fig. S4 and S5, ESI‡). Nevertheless, the highest nitrogen uptake at 77 K at 1 bar could be reached with DUT-79 (Fig. S11–S14, ESI‡). The BET surface area and pore volume derived from the isotherm is 980 $m^2\ g^{-1}$ and 0.59 $cm^3\ g^{-1}$, respectively.

Conclusions

In summary, using trigonal and square-planar building blocks, the topology of the resulting frameworks can be controlled either by addition of topology directing agents or by varying the conformational degree of freedom in the trigonal ligand. This concept exemplified producing of five novel materials namely DUT-63, DUT-64, DUT-77, DUT-78, and DUT-79. In the case of conformationally labile H_3tcbpa, the formation of framework polymorphs makes the prediction of resulting compound difficult. For conformationally restricted ligands such as H_3hmbqa, only **pto** frameworks could be obtained under conditions investigated. Moreover, post synthetic functionalization of DUT-64 and DUT-78 by Cu(salen) ligand leads to the interconnection of the paddle-wheels with the formation of **ith-d** net within DUT-78 and DUT-79 materials. We believe that this could improve the application potential for these MOFs in the heterogeneous catalysis, light emitting devices and other functional systems.

Acknowledgements

The HZB is gratefully acknowledged for the allocation of the synchrotron radiation beam time on MX BL14.2 and BL14.3 beamlines and for travel grants. VB is thankful to German Federal Ministry of Education and Research for the financial support (Project BMBF No 05K16OD1). MP acknowledges financial support by the ERC grant 2DMATER and the EC under the Graphene Flagship (grant number CNECT-ICT-604391).

References

1 M. Eddaoudi, D. B. Moler, H. Li, B. Chen, T. M. Reineke, M. O'Keeffe and O. M. Yaghi, *Acc. Chem. Res.*, 2001, **34**, 319.
2 *Chem. Rev.*, 2012, Special Issue on MOFs.
3 *Chem. Soc. Rev.*, 2014, Special Issue on MOFs.
4 M. A. Addicoat, D. E. Coupry and T. Heine, *J. Phys. Chem. A*, 2014, **118**, 9607.
5 C. E. Wilmer, M. Leaf, C. Y. Lee, O. K. Farha, B. G. Hauser, J. T. Hupp and R. Q. Snurr, *Nat. Chem.*, 2012, **4**, 83.
6 M. Li, D. Li, M. O'keeffe and O. M. Yaghi, *Chem. Rev.*, 2013, **114**, 1343.
7 M. O'keeffe and O. M. Yaghi, *Chem. Rev.*, 2011, **112**, 675.
8 N. Klein, I. Senkovska, I. A. Baburin, R. Grünker, U. Stoeck, M. Schlichtenmayer, B. Streppel, U. Mueller, S. Leoni, M. Hirscher and S. Kaskel, *Chem. – Eur. J.*, 2011, **17**, 13007.
9 D. Tian, Q. Chen, Y. Li, Y.-H. Zhang, Z. Chang and X.-H. Bu, *Angew. Chem., Int. Ed.*, 2014, **53**, 837.
10 H. Wang, J. Xu, D.-S. Zhang, Q. Chen, R.-M. Wen, Z. Chang and X.-H. Bu, *Angew. Chem., Int. Ed.*, 2015, **54**, 5966.
11 S. S.-Y. Chui, S. M.-F. Lo, J. P. H. Charmant, A. G. Orpen and I. D. Williams, *Science*, 1999, **283**, 1148.
12 M. Eddaoudi, J. Kim, N. Rosi, D. Vodak, J. Wachter, M. O'keeffe and O. M. Yaghi, *Science*, 2002, **295**, 469.
13 I. Senkovska and S. Kaskel, *Chem. Commun.*, 2014, **50**, 7089.
14 K. Gedrich, M. Heitbaum, A. Notzon, I. Senkovska, R. Fröhlich, J. Getzschmann, U. Mueller, F. Glorius and S. Kaskel, *Chem. – Eur. J.*, 2011, **17**, 2099.
15 D. Sun, S. Ma, Y. Ke, D. J. Collins and H.-C. Zhou, *J. Am. Chem. Soc.*, 2006, **128**, 3896.
16 S. Ma, D. Sun, M. Ambrogio, J. A. Fillinger, S. Parkin and H.-C. Zhou, *J. Am. Chem. Soc.*, 2007, **129**, 1858.
17 H. Furukawa, Y. B. Go, N. Ko, Y. K. Park, F. J. Uribe-Romo, J. Kim, M. O'keeffe and O. M. Yaghi, *Inorg. Chem.*, 2011, **50**, 9147.
18 N. Zhu, M. J. Lennox, T. Düren and W. Schmitt, *Chem. Commun.*, 2014, **50**, 4207.
19 S. Bureekaew and R. Schmid, *CrystEngComm*, 2013, **15**, 1551.
20 H. J. Park, D.-W. Lim, W. S. Yang, T.-R. Oh and M. P. Suh, *Chem. – Eur. J.*, 2011, **17**, 7251.
21 Y.-P. He, Y.-X. Tan and J. Zhang, *Chem. Commun.*, 2013, **49**, 11323.
22 Y.-P. He, Y.-X. Tan and J. Zhang, *Inorg. Chem.*, 2013, **52**, 12758.
23 D. Shi, Y. Ren, H. Jiang, B. Cai and J. Lu, *Inorg. Chem.*, 2012, **51**, 6498.

24 D. De, S. Neogi, E. C. Sañudo and P. K. Bharadwaj, *Chem. – Eur. J.*, 2015, **21**, 17422.
25 Y.-P. He, Y.-X. Tan and J. Zhang, *J. Mater. Chem. C*, 2014, **2**, 4436.
26 Y.-P. He, Y.-X. Tan and J. Zhang, *Cryst. Growth Des.*, 2013, **13**, 6.
27 Y.-P. He, Y.-X. Tan, F. Wang and J. Zhang, *Inorg. Chem.*, 2012, **51**, 1995.
28 Y.-P. He, Y.-X. Tan and J. Zhang, *Inorg. Chem.*, 2015, **54**, 6653.
29 Y.-X. Tan, Y.-P. He and J. Zhang, *Cryst. Growth Des.*, 2012, **12**, 2468.
30 B. Chen, X. Zhao, A. Putkham, K. Hong, E. B. Lobkovsky, E. J. Hurtado, A. J. Fletcher and K. M. Thomas, *J. Am. Chem. Soc.*, 2008, **130**, 6411.
31 Z. Fang, T.-L. Teo, L. Cai, Y.-H. Lai, A. Samoc and M. Samoc, *Org. Lett.*, 2009, **11**, 1.
32 T. F. Willems, C. H. Rycroft, M. Kazi, J. C. Meza and M. Haranczyk, *Microporous Mesoporous Mater.*, 2012, **149**, 134.
33 U. Mueller, N. Darowski, M. R. Fuchs, R. Forster, M. Hellmig, K. S. Paithankar, S. Puhringer, M. Steffien, G. Zocher and M. S. Weiss, *J. Synchrotron Radiat.*, 2012, **19**, 442.
34 M. D. Winn, C. C. Ballard, K. D. Cowtan, E. J. Dodson, P. Emsley, P. R. Evans, R. M. Keegan, E. B. Krissinel, A. G. W. Leslie, A. Mccoy, S. J. Mcnicholas, G. N. Murshudov, N. S. Pannu, E. A. Potterton, H. R. Powell, R. J. Read, A. Vagin and K. S. Wilson, *Acta Crystallogr., Sect. D: Biol. Crystallogr.*, 2011, **67**, 235.
35 G. Sheldrick, *Acta Crystallogr., Sect. A: Found. Crystallogr.*, 2008, **64**, 112.
36 A. Spek, *J. Appl. Crystallogr.*, 2003, **36**, 7.
37 P. Müller, F. M. Wisser, V. Bon, R. Grünker, I. Senkovska and S. Kaskel, *Chem. Mater.*, 2015, **27**, 2460.
38 M. Xue, S. Ma, Z. Jin, R. M. Schaffino, G.-S. Zhu, E. B. Lobkovsky, S.-L. Qiu and B. Chen, *Inorg. Chem.*, 2008, **47**, 6825.
39 H. Chung, P. M. Barron, R. W. Novotny, H.-T. Son, C. Hu and W. Choe, *Cryst. Growth Des.*, 2009, **9**, 3327.
40 H. Zhao, D. Jia, J. Li, G. J. Moxey and C. Zhang, *Inorg. Chim. Acta*, 2015, **432**, 1.
41 *Material Studio 5.0*, Accelrys Software Inc, San Diego, USA, 2009.
42 A. A. Talin, A. Centrone, A. C. Ford, M. E. Foster, V. Stavila, P. Haney, R. A. Kinney, V. Szalai, F. El Gabaly, H. P. Yoon, F. Léonard and M. D. Allendorf, *Science*, 2014, **343**, 66.